# EVALUATION OF MACHINING DAMAGE AROUND DRILLED HOLES IN CFRPS USING MICRO-RAMAN SPECTROSCOPY

T. Miyake[1*], T. Tanaka[1], M. Ftamura[2]

[1]*Department of Mechanical and Systems Engineering, Gifu University, 1-1 Yanagido Gifu 501-1193, Japan*
[2]*Nagoya Municipal Industrial Research Institute, 3-4-41 Rokuban Atsuta-ku Nagoya 456-0058, Japan*
**miyake@gifu-u.ac.jp*

**Keywords:** machining damage, CFRPs, drilled hole, micro-Raman spectroscopy

**Abstract**
*Joining accompanied with drilling is widely used to assemble CFRP composites in aerospace industries. Although drilling-induced microscopic damage in CFRP composites is closely related with long-term performance deterioration, there is no applicable method to evaluate them. Noticing that machining micro-damage appears as fiber-matrix interfacial debonding and interfacial debonding can be determined in μm order special resolution from the fiber stress distribution obtained using micro-Raman spectroscopy, extent of drilling damage was investigated experimentally for individual fibers around the drilled hole by micro-Raman spectroscopy. As a result, range of interfacial debonding is proved to differ with the fiber location, whether on the drill-entry side or the drill-exit side, and the fiber orientation to the drill cutting-edge rotation.*

## 1 Introduction

Fastening by means of fasteners is widely used to join CFRP parts with metal parts in aircraft structures. It requires the drilling of large number of holes in CFRPs. However CFRP composites are difficult-to-machine materials, which result in drilling-induced damage [1]. However drilling-induced damage significantly reduces bearing strength of the composites, only macroscopic damage, e.g. chipping or delamination can be observed [2,3]. Whereas, microscopic damage, e.g. micro-cracking or fiber/matrix debonding have the potential for long-term performance deterioration as well, but there is no method to detect. Studies on fiber stress measurement using micro-Raman spectroscopy have proved that stress distribution in the fiber of composites depends on the interfacial bonding between fiber and matrix [4]. Suppose fiber-matrix debonding is associated with drilling, local stress measurement by micro-Raman spectroscopy could evaluate drilling-associated micro defects in special resolution of μm order.

The present study attempts to clarify quantitatively the detail of fiber-matrix debonding caused by drilling in μm special resolution. Difference in debonding range between at the entry and at the exit of drilled holes periphery was examined. Dependence of fiber orientation relative to the drill cutting-edge rotation on the interfacial debonding was also investigated by measuring stress distribution of fibers located at angles of 0°, 90° and 180° with the fiber-orientation of unidirectional composites.

## 2 Experimental procedure

### *2.1 Materials and specimens*

The composite materials used for the drilling tests were unidirectional carbon fiber/epoxy matrix ones fabricated using VaRTM molding, as shown in figure 1. The CFRP laminates were 1mm thick and have 60% cured fiber volume fraction. The fibers employed were high modulus PAN-based carbon fibers (M46JB-12K TORAY Ind. Inc.). After drilling under the condition as stated below, the composite panel was cut into strip specimens shown in figure 2 for micro-Raman measurement.

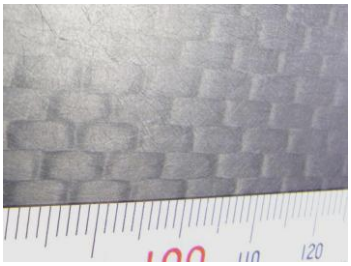

**Figure 1.** Unidirectional CFRP laminates.

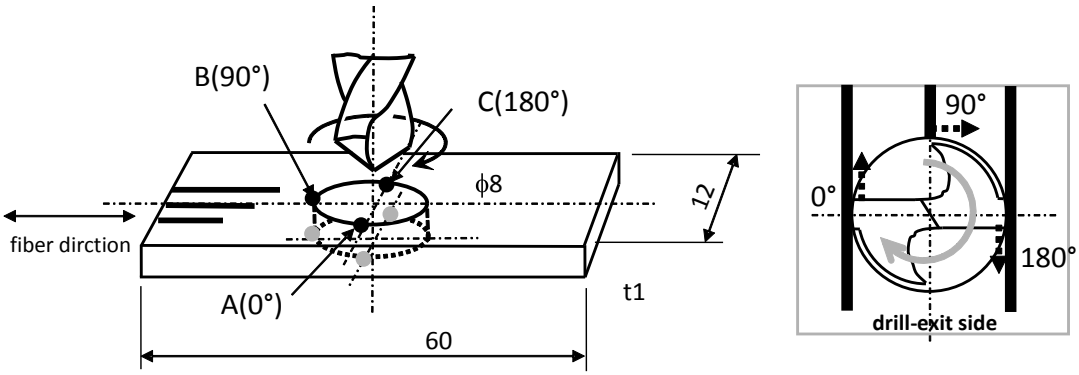


**Figure 2.** Shape of specimens and Raman measurement points.

### *2.2 Drill and drilling condition*

All drilling experiments were carried out using custom-built tools of 8 mm diameter with two cutting edges, as shown in figure 3, which were coated polycrystalline diamond (PCD). Drilling was done under dry condition with air cooling by utilizing the hollow shaft of the drill. Table 1 shows the drilling condition.

**Figure 3.** Drill employed with hollow shaft.

| | |
|---|---|
| **Feed (mm/sec.)** | **1** |
| **Rotational speed (r.p.m.)** | **2,000** |

**Table 1.** Drilling condition.

### *2.3 Evaluation of drill-induce damage (fiber-matrix interfacial debonding)*

Figure 4 schematically shows stress distribution of fiber embedded in matrix under tensile loading. As shown in the figure, fiber stress distribution depends on the interfacial bonding,

i.e. whether perfect bonding or debonding between fiber and matrix. If debonding is caused at the interface, shear stress does not transfer from the matrix to the fiber and the fiber is not stressed. The debonding range can be exactly determined from the fiber stress distribution.

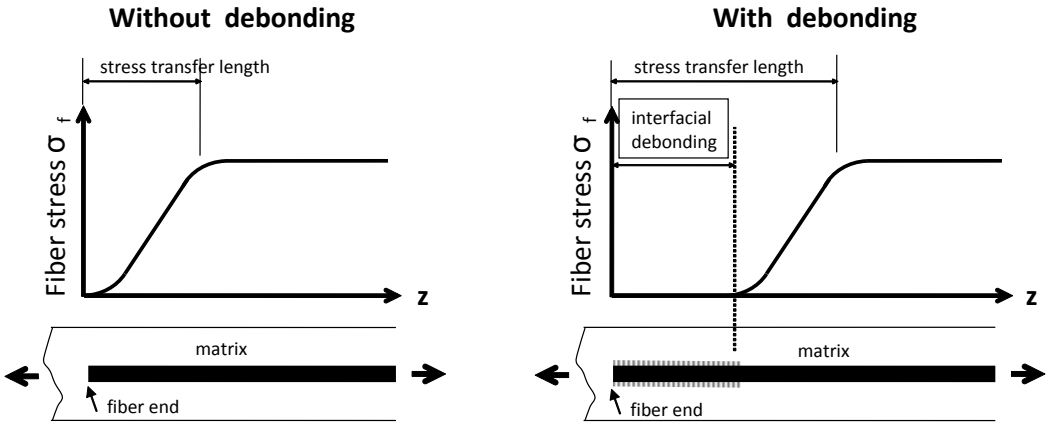


**Figure 4.** Fiber stress distribution under tension with and without interfacial debonding.

*2.4 Micro-Raman measurement*

Stress measurement by micro-Raman spectroscopy was carried out for fibers around the drilled holes under tensile loading by mean of a rig which was mounted directly on the microscope stage in the Raman system, as shown in figure 5. Tensile stress was not induced in the fiber due to the presence of the drilled hole, and then the holes were filled again by epoxy resin to apply tensile stress for the Raman measurement.

**Figure 5.** Micro-Raman spectroscope with a custom-made loading rig.

Raman spectra were measured by a micro-Raman spectrometer system (LabRAM-300 Jobin Yvon), which was consisted of a 300mm polychromater. He-Ne laser light at a wavelength of 633nm was focused to a 1-μm diameter spot on the fiber surface by an optical microscope lens at 100× magnification and the back-scattered light was collected by the same lens. The Raman spectroscopy measurement condition was listed at Table 2.

| | |
|---|---|
| **Laser** | **He-Ne 633nm** |
| | **<1mW on specimen surface** |
| **Objective lens** | **100×** |
| **Exposure time** | **30sec.** |

**Table 2.** Micro-Raman measurement conditions.

Measurement of Raman spectroscopy was carried out at the 6 locations shown in figure 1, both before and after tensile loading. Measuring points were called 0°, 90° and 180° respectively depending on the angle between the fiber orientation and the drill cutting-edge motion. Fibers located at the periphery of drill-entry and dill-exit side were also measured in the same way. In order to obtain fiber stress distribution specimens were translated in the fiber direction by the intervals shown in figure. 6.

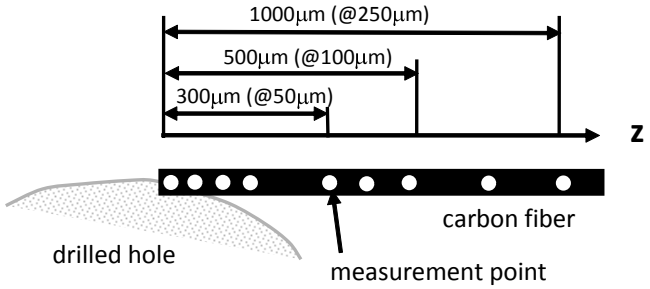


**Figure 6.** Micro-Raman spectroscopy measurement points to obtain fiber stress distribution.

Measurements were replicated at the same points on the fibers before and after loading, and change in the fiber stress was examined. Three adjacent fibers embedded about 5μm deep were measured to see the variation on fibers.

## 3 Results

### *3.1 Stress evaluation by Raman spectra*

The Raman peak of wave number of 2700cm$^{-1}$, D'-band, was used to evaluate the fiber stress, because the other two peaks from the fiber, D-band (1350 cm$^{-1}$) and G-band(1580cm$^{-1}$), was found to be overlapped with the Raman peaks from the resin [5]. Figure 7 shows the dependence of peak wave number on applied stress, which was obtained from a stressed free-standing fiber. They are almost in a linear relation and fiber stress can be estimated from the peak wave number using the relation.

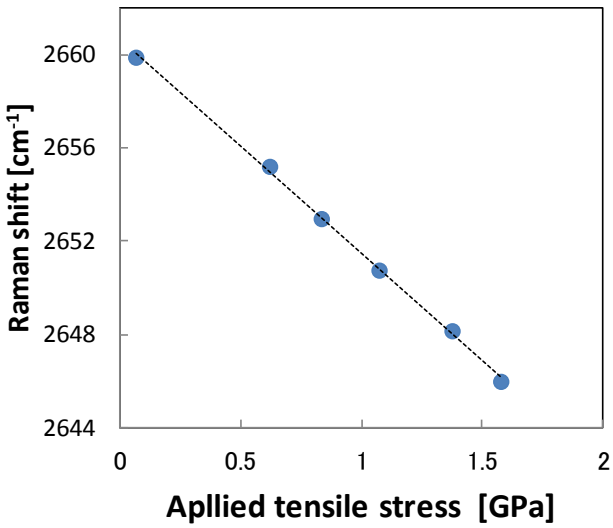


**Figure 7.** Dependence of D' band peak wave number on applied tensile stress.

*3.2 Stress distribution of fiber at drilled holes periphery*

First, it is verified that the fibers in the drill hole-filled specimen were stressed by loading. As shown in figure 8, 5 points on the fibers within ±100μm around the center line of the specimen, at 2 mm far from the hole-edge showed almost the same variation by tensile load.

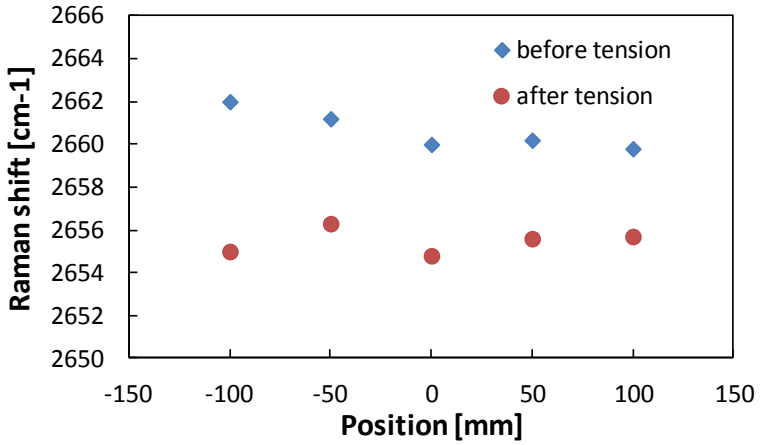


**Figure 8.** Raman shift due to tensile stress in the fibers of hole-filled specimen with tensile loading.

*(a) At position 0° (up-cut direction) of drill-exit side*

Figure 9 showed the fiber stress distribution under tensile load at 0° of the drill-exit side. The shown result was one of the three measurements carried out. From the figure fiber stress was found to be zero at the edge and increase with the distance z from the edge up to almost the constant stress at z > 500μm. However, it was noticed that fiber stress was not almost caused at 0 < z < 150μm.

*(b) At position 180° (down-cut direction) of drill-entry side*

The fiber stress distribution at 180° of the drill-entry side when the specimen was loaded was shown in figure 10. Although the fiber stress showed a similar distribution as that at position 0°, but it increased monotonously from z = 0 with z except the fluctuation around z = 200-300μm. Such range that fiber stress was not caused seen in the 0° experiment, was not observed in this case.

*3.3 Discussion*

The former mentioned case (a) and (b) were performed using different specimens and the resultant settling stresses were different from each other. Compared with the both results in figure 11, almost the same stress build-up was seen in the region of z > 250-300μm. On the other hand, in the region of 50μm < z < 200μm the stress distributions considerably differed from each other. In the result of case (a), stress was not almost caused z < 150μm and this resulted that the stress build-up in the case of (a) shifted about 100μm longer in the distance z compared to that of the case (b). From these results and the schematic model shown in figure 4, it was considered that perfect debonding about 100μm long was occurred at the fiber-matrix interface in the case (a). In case of (b) the debonding might occur in z < 50μm.

Because the case (a) and the case (b) were far different in location relative to the slope of drill bit flutes and the rotation of drill bit cutting-edges, fiber location was considered to be responsible for interfacial debonding.

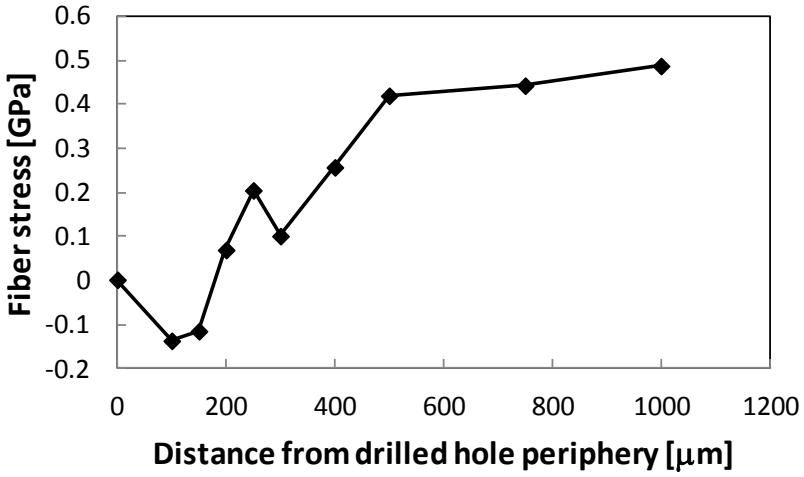


**Figure 9.** Stress distribution in the fiber located at 0° (up-cut direction) of drill-exit side.

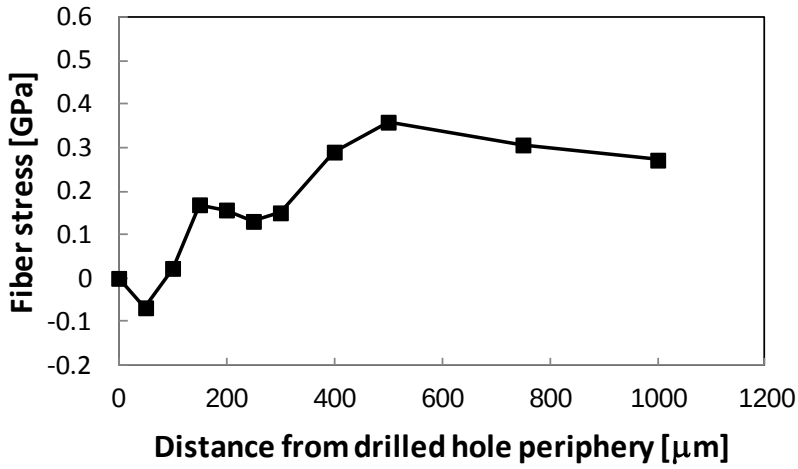


**Figure10.** Stress distribution in the fiber located at 180° (down-cut direction) of drill-entry side.

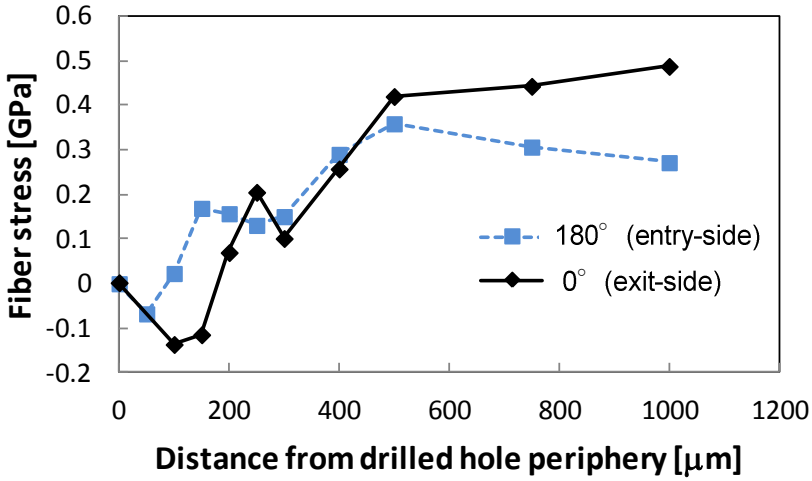


**Figure11.** Comparison of Stress distribution in the fiber located at 0° (up-cut direction) of drill-exit side and at. 180° (down-cut direction) of drill-entry side.

## 4 Conclusions

In the present study, quantitative evaluation of drilling-induced damage in unidirectional composites was attempted by means of detecting the resulting fiber-matrix debonding using micro-Raman spectroscopy. Locality in drilling-induced damage was investigated by the dependence of damaged range on fiber location to drill feed and orientation relative to drill cutting-edge. The results obtained are as follows:

- Measurement by micro-Raman spectroscopy clarified the range of the fiber-matrix interfacial debonding, which was supposed to be caused due to drilling.
- Interfacial debonding range over 100μm long was detected in the fiber of the drill-exit side located at an angle of 0° to the drill cutting-edge rotation. On the other hand, debonding was hardly detected in the fiber of the drill-entry side at an angle of 180°.
- The method presented in the study is useful to estimate quantitatively machining damage in CFRP composites and is also available to develop damage-free drills or drilling conditions.

## References

[1] Liu D., Tang Y., Cong W.L. A review of mechanical drilling for composite laminates. Compos. Struct., **94**, pp.1265-1279 (2012).

[2] Khashaba U.A. Delamination in drilling GFR-thermoset composites. Compos. Struct., **63**, pp.313-326 (2004).

[3] Jahromi A.S., Gudimani G., Kalla D.K., Bahr B. Effect of high RPM machining and fiber orientation on subsurface damage in machining of unidirectional composites in "Proceeding of SAMPE 2011", Long Beach, USA, (2011).

[4] Galiotis C. A study of mechanisms of stress transfer in continuous- and discontinuous-fibre model composites by laser Raman spectroscopy, Compos. Sci. Technol., **48**, pp.15-28 (1993).

[5] Miyake T., Yamakawa T., Ohno N. Measurement of stress relaxation in broken fibers embedded in epoxy using Raman spectroscopy, J. Mater. Sci., **33**, pp.5177-5183 (1998).